HHS Public Access

Author manuscript

Science. Author manuscript; available in PMC 2020 July 01.

Published in final edited form as:

Science. 2019 August 09; 365(6453): 599–604. doi:10.1126/science.aax3649.

A dominant-negative effect drives selection of *TP53* missense mutations in myeloid malignancies

Steffen Boettcher[1,2,3], **Peter G. Miller**[1,2,3], **Rohan Sharma**[2,3], **Marie McConkey**[2,3], **Matthew Leventhal**[2,3], **Andrei V. Krivtsov**[4], **Andrew O. Giacomelli**[1,2,5], **Waihay Wong**[2,3], **Jesi Kim**[3], **Sherry Chao**[2,6], **Kari J. Kurppa**[1,7], **Xiaoping Yang**[2], **Kirsten Milenkowic**[2], **Federica Piccioni**[2], **David E. Root**[2], **Frank G. Rücker**[8], **Yael Flamand**[9], **Donna Neuberg**[9], **R. Coleman Lindsley**[1,2], **Pasi A. Jänne**[1,7], **William C. Hahn**[1,2], **Tyler Jacks**[10,11,12], **Hartmut Döhner**[8], **Scott A. Armstrong**[4], **Benjamin L. Ebert**[1,2,3,13,*]

[1]Dana-Farber Cancer Institute, Department of Medical Oncology, Boston, MA 02215, USA.

[2]Broad Institute of MIT and Harvard, Cambridge, MA 02142, USA.

[3]Brigham and Women's Hospital, Division of Hematology, Harvard Medical School, Boston, MA 02115, USA.

[4]Dana-Farber Cancer Institute, Department of Pediatric Oncology, Boston, MA 02215, USA.

[5]The Campbell Family Institute for Breast Cancer Research, Princess Margaret Cancer Centre, University Health Network, Toronto, ON M5G 2M9, Canada.

[6]Department of Biomedical Informatics, Harvard University, Boston, MA 02115, USA.

[7]Dana-Farber Cancer Institute, Belfer Center for Applied Cancer Science, Boston, MA 02215, USA.

[8]Department of Internal Medicine III, University of Ulm, Ulm, Germany.

[9]Dana-Farber Cancer Institute, Department of Biostatistics and Computational Biology, Boston, MA 02215, USA.

[10]David H. Koch Institute for Integrative Cancer Research, Massachusetts Institute of Technology, Cambridge, MA, 02139, USA.

[11]Department of Biology, Massachusetts Institute of Technology, Cambridge, MA, 02139, USA.

[*]Corresponding author. benjamin_ebert@dfci.harvard.edu (B.L.E.).

Author contributions: S.B. devised and conducted experiments and wrote the manuscript. P.G.M., R.S., M.M., M.L., W.W., J.K., S.C., K.J.K., R.C.L., P.A.J., and T.J. helped with experiments, provided reagents and analyzed data. A.O.G., W.C.H., X.Y., K.M., F.P., and D.E.R helped perform and analyze the *TP53* saturation mutagenesis screen. A.V.K. and S.A.A. helped perform and analyze ChIP-seq and RNA-seq analyses. H.D. and F.G.R. provided, Y.F. and D.N. analyzed *TP53* mutational and clinical data from patients with AML. B.L.E. directed the study and wrote the manuscript. All authors contributed to writing of the manuscript.

Competing interests: P.G.M. receives consulting fees from Foundation Medicine, Inc. WCH is a consultant for ThermoFisher, Parexel, AjuIB, and MPM and is a founder and advisor to KSQ Therapeutics. S.A.A. has been a consultant and/or shareholder for Epizyme Inc, Imago Biosciences, Cyteir Therapeutics, C4 Therapeutics, Syros Pharmaceuticals, OxStem Oncology, Accent Therapeutics and Mana Therapeutics. S.A.A. has received research support from Janssen, Novartis, and AstraZeneca. B.L.E. has been a consultant for Grail and has received research support from Celgene and Deerfield.

Data and materials availability: ChIP-seq and RNA-seq data are being made accessible at the Gene Expression Omnibus (GEO) database repository GSE131484 (ChIP-seq) and GSE131592 (RNA-seq). Materials are available from B.L.E. upon request.

[12]Howard Hughes Medical Institute, Massachusetts Institute of Technology, Cambridge, MA, 02139, USA.

[13]Howard Hughes Medical Institute, Dana-Farber Cancer Institute, Boston, MA, 02215, USA.

Abstract

TP53, which encodes the tumor suppressor p53, is the most frequently mutated gene in human cancer. The selective pressures shaping its mutational spectrum, dominated by missense mutations, are enigmatic, and neomorphic gain-of-function (GOF) activities have been implicated. We used CRISPR/Cas9 to generate isogenic human leukemia cell lines of the most common *TP53* missense mutations. Functional, DNA binding, and transcriptional analyses revealed loss-of-function (LOF) but no GOF effects. Comprehensive mutational scanning of p53 single amino acid variants demonstrated that missense variants in the DNA-binding domain exert dominant-negative effects (DNE). In mice, the DNE of p53 missense variants confer a selective advantage to hematopoietic cells upon DNA damage. Analysis of clinical outcomes in acute myeloid leukemia patients showed no evidence of GOF for *TP53* missense mutations. Thus, dominant-negative effects are the primary unit of selection for *TP53* missense mutations in myeloid malignancies.

The transcription factor p53, encoded by its gene *TP53,* is a tumor suppressor involved in the response to pathogenic stimuli such as DNA damage, oxidative stress, and oncogenic hyperproliferation (1). *TP53* is the most frequently mutated gene in human cancer. *TP53*-mutant acute myeloid leukemia (AML) and myelodysplastic syndromes (MDS) have an extremely poor prognosis (2), are often refractory to chemotherapy (3) and have a high rate of relapse after allogeneic hematopoietic stem cell transplantation (4).

About 80% of mutations in *TP53* across all cancer subtypes are protein-altering missense mutations that occur within its DNA-binding domain, clustering at several hotspot amino acid residues (5). Loss of heterozygosity is a common but not mandatory event during clonal evolution of tumors with *TP53* missense mutations (6). This unusual mutational spectrum for a tumor suppressor gene, which normally undergo biallelic inactivation, has led to the hypothesis that p53 missense mutants may be selected for due to an oncogenic gain-of-function (GOF) (7, 8). Supporting evidence comes from *in vitro* and *in vivo* studies in mice that have demonstrated higher oncogenic potential of $p53^{missense}$ tumors as compared to $p53^{null}$ tumors (9, 10). Mutant p53 has been shown to engage in novel protein-protein interactions with other transcription factors resulting in abnormal tumor-promoting transcriptional programs (11-15). An alternative hypothesis is that selection for *TP53* missense mutations may be due to dominant-negative effects (DNE), leading to non-mutational impairment of the remaining wild-type allele (16-19). While mutant p53 pathophysiology has largely been studied in epithelial cancers, with a focus on solid tumor phenotypes such as migration, invasion, and metastasis, the effects of *TP53* missense mutations within the hematopoietic system have been investigated less thoroughly. The selective forces shaping the mutational spectrum of *TP53* in myeloid malignancies have remained elusive but may be relevant for rational design of therapies aimed at preventing clonal selection of *TP53*-mutant clones. We sought to elucidate the functional consequences of *TP53* missense mutations in myeloid malignancies using a series of isogenic cellular

models, facilitated by advances in genome editing that enable systematic examination of mutant alleles.

We identified the six most frequent *TP53* missense mutations (Fig. S1) in the largest cohort of high-risk MDS patients analyzed to date (4) and introduced these mutations, along with null alleles, into two independent human AML cell line models using CRISPR/Cas9 genome-editing (Fig. 1A, Fig. S2A, Fig. S3A). These isogenic cell lines allow comparison of mutant, wild-type and null alleles expressed from the endogenous locus, leaving the full complexity of p53 feedback mechanisms intact. We generated K562-*TP53* isogenic cells by repairing the hemizygous $TP53^{Q136fs}$ mutation in parental K562, which reactivated wild-type p53 activity in the K562 cells, and then introducing *TP53* missense and null mutations (Fig. S2A-C, table S1). In the AML cell line MOLM13 that carries two wild-type *TP53* copies, missense and null mutations were introduced into one or both endogenous loci (Fig. S3A, table S2).

We characterized these isogenic cell lines with allelic series of *TP53* genotypes in various functional assays. Assessment of cell cycle status and apoptosis after DNA damage revealed intact functionality of these p53-regulated pathways in wild-type *TP53* K562 and MOLM13 isogenic cells (Fig. 1B, Fig. S2D, Fig. S3B) with the exception of a previously described (20) intrinsic apoptotic defect in parental K562 cells (Fig. S2E, F). *TP53*-mutant MOLM13 isogenic cells were relatively resistant to apoptosis (Fig. 1B), and both *TP53*-mutant MOLM13 and K562 isogenic cells failed to arrest in G1 (Fig. S2D, Fig. S3B). In both isogenic cell line models, the abundance of p53 protein, in steady-state and upon daunorubicin-induced DNA damage, was influenced by specific mutations (Fig. 1C, Fig. S2G). Furthermore, in contrast with previous studies in which overexpression of wild-type p53 in $TP53^{null}$ cancer cell lines resulted in decreased proliferation (21-23), expression of wild-type or mutant p53 from the endogenous locus did not affect cell proliferation under steady-state conditions in either cell line model (Fig. 1D, Fig. S2H).

MOLM13-TP53 cells with either missense or null alleles were equally resistant to daunorubicin-induced apoptosis (Fig. 1B), and accordingly, both $TP53^{missense/-}$ and $TP53^{-/-}$ cells were equally more resistant to chemotherapeutics than $TP53^{+/+}$ cells (Fig. 1E). This translated into a sustained competitive advantage over $TP53^{++}$ cells, as determined by *in vitro* mixing experiments (Fig. S4A-C). Consequently, no competitive fitness difference was observed when *TP53* missense mutant cells were co-cultured with *TP53* null cells in the presence of dimethyl sulfoxide (DMSO) or daunorubicin (Fig. S5A-C). The slight increase in percentage of $TP53^{Y220C/-}$ and $TP53^{M237I/-}$ cells relative to $TP53^{-/-}$ cells in MOLM13 isogenic cells (Fig. S5B) but not K562 isogenic cells (Fig. S5C) was therefore considered to be due to subtle differences in proliferative capacities between isogenic MOLM13 lines. Collectively, *TP53* isogenic AML cell lines generated by CRISPR/Cas9 genome-editing not only faithfully recapitulate p53 biology, but also revealed that cells with *TP53* missense and null alleles show the same oncogenic phenotypes *in vitro* with respect to proliferative capacity, decreased apoptotic potential, lack of G1 cell cycle arrest, and resistance to cytotoxic agents.

The vast majority of *TP53* missense mutations affect p53's DNA-binding domain, which raises the possibility that they result in activation of *de novo* transcriptional programs. We therefore performed chromatin immunoprecipitation sequencing (ChIP-seq) and RNA-seq analyses in both isogenic cell line models in steady-state and after DNA damage. First, we determined enrichment of wild-type or missense mutant p53 binding relative to the p53 null state, which served as control. As expected, we observed strong enrichment of wild-type p53 binding to promoter regions in both DMSO- and daunorubicin-treated samples (Fig. 2A, Fig. S6A). In contrast, three of six missense mutants (R175H, R248Q, R273H) lost nearly all DNA-binding activity. Two mutants (Y220C and M237I) had decreased but residual DNA binding, with the target sites almost completely overlapping those found in cells with wild-type p53 and with no evidence for novel binding sites (Fig. 2A, Fig. S6A-C). The R282W mutant had increased promoter occupancy, maintaining wild-type-like DNA-binding activity while also acquiring novel binding sites (Fig. 2A, Fig. S6A-C).

Since promoter occupancy is necessary but not sufficient to transactivate expression of p53 target genes, we examined whether promoter binding of wild-type or mutant p53 results in expression of the associated genes (Fig. 2B, Fig. S7A-C). As expected, genes associated with wild-type-specific ChIP-seq peaks were expressed at higher levels in cells with wild-type *TP53* compared to cells with missense mutant or null alleles (Fig. 2B left, Fig. S7C left). Even genes associated with ChIP-seq peaks shared between wild-type and missense mutant p53 were expressed at much higher levels in cells with wild-type *TP53* as compared to cells with missense mutant or null alleles (Fig. 2B middle, Fig. S7C middle). In contrast, genes associated with missense mutant-specific ChIP-seq peaks, most of which were contributed by R282W mutant, were not differentially expressed between cells with *TP53* missense mutant, null or wild-type alleles (Fig. 2B right, Fig. S7C right). These data indicate that p53 missense mutants are not capable of activating gene expression, including at *de novo* sites of p53 R282W mutant binding, even upon exposure to chemotherapy.

To examine the possibility that missense mutant p53 drives an oncogenic GOF transcriptional program independent of its ability to directly act as a transcriptional activator or repressor, we analyzed our RNA-seq data without considering results from the ChIP-seq experiments. In contrast to prior reports that common p53 missense variants exert a universal transcriptional GOF (14, 15), we found no indication of a common p53 missense mutant-driven GOF transcriptional program in either isogenic model, in steady-state or upon daunorubicin-induced DNA damage (Fig. 2C, Fig. S8A-C). We did, however, identify a strong transcriptional signature of genes that have increased expression in *TP53* wild-type cells after DNA damage and that have lower expression in *TP53*-mutant cells. Notably, this signature was shared by all *TP53* missense and null mutant cells but not by *TP53* wild-type cells (Fig. 2C, Fig. S8A-C). This result emphasizes that the dominant gene expression signature of cells carrying *TP53* missense mutations is the signature of *TP53* inactivation, as demonstrated by equivalency to the transcriptional state of $TP53^{null}$ cells. Accordingly, gene ontology analysis performed on the 30 most differentially expressed genes revealed biological processes closely associated with p53-regulated pathways, such as apoptosis and cell cycle regulation, to be the most altered in cells with *TP53* missense mutant or null alleles (Fig. S8D, Fig. S9A, B).

As noted above, dominant-negative effects (DNE) provide an alternative explanation to GOF mechanisms as a biological basis for the selective pressure for specific missense mutations (16-19). To test for DNE, we used CRISPR/Cas9 genome editing to generate isogenic MOLM13 cell lines with an allelic series that comprises *TP53*$^{+/+}$, *TP53*$^{+/-}$, *TP53*$^{-/-}$, *TP53*$^{R248Q/+}$, and *TP53*$^{R248Q/-}$. We used *CDKN1A* and p21 expression as a surrogate marker for p53 functionality. Daunorubicin treatment led to an increase in *CDKN1A* mRNA and p21 protein levels in *TP53*$^{+/+}$ and *TP53*$^{+/-}$ cells but not in *TP53*$^{-/-}$, *TP53*$^{R248Q/+}$, and *TP53*$^{R248Q/-}$ cells (Fig. 3A, Fig. S10A). These results demonstrate that in heterozygous cells with endogenous expression of p53^{R248Q} from one allele and endogenous p53$^{wild\text{-}type}$ from the other allele, the missense variant inhibits transcriptional activity of the wild-type p53 protein in a dominant-negative manner. Consequently, *TP53*$^{R248Q/+}$ cells showed a greater functional impairment of p53-dependent G1 cell cycle arrest and apoptosis upon daunorubicin treatment than *TP53*$^{+/-}$ cells (Fig. 3B, Fig. S10B). Moreover, *TP53*$^{-/-}$, *TP53*$^{R248Q/+}$, and *TP53*$^{R248Q/-}$ cells were functionally equivalent as demonstrated by an equal degree of resistance to daunorubicin or nutlin-3a, an inhibitor of MDM2-mediated proteasomal degradation of p53, compared to *TP53*$^{+/+}$ and *TP53*$^{+/-}$ cells (Fig. 3C). Similarly, both *TP53*$^{R248Q/+}$ and *TP53*$^{R248Q/-}$ cells rapidly outcompeted *TP53*$^{+/+}$ cells in co-culture assays in the presence of nutlin-3a (Fig. S10C). Collectively, these data demonstrate that p53^{R248Q} exerts a DNE on the functionality of p53$^{wild\text{-}type}$ in heterozygous AML cells, leading to enhanced competitive fitness of *TP53*$^{R248Q/+}$ compared to *TP53+/–* cells after DNA damage.

We next sought to examine all potential *TP53* missense mutations in an unbiased fashion. To this end, we performed a saturation mutagenesis screen in which each amino acid in p53 was systematically mutated to all other possible amino acids and a stop codon, as previously described (24). We introduced this pool of *TP53*-mutant cDNAs into a novel reporter AML cell line with wild-type p53 activity that was engineered to express a p21-green fluorescent protein (GFP) fusion protein from the endogenous *CDKN1A* locus. This enabled us to monitor by flow cytometry the biochemical consequences of p53 missense variants on wild-type p53's transcriptional activity (Fig. S11A, B). Reporter cells expressing the mutant cDNAs were treated with nutlin-3a to induce p53, and cells were sorted and sequenced on the basis of p21-GFP expression (Fig. S11C). Amino acid substitutions at residues 100-300, encompassing the DNA-binding domain, were powerfully enriched for dominant-negative activity both in DMSO- and nutlin-3a-treated reporter cells (Fig. 3D, Fig. S11D). The amino acid substitutions resulting in DNE in our functional screen are highly concordant with missense *TP53* mutations in a cohort of 1,040 patients with myeloid malignancies (Fig. 3D). Two saturation mutagenesis studies conducted in solid tumor models have recently reported conflicting results supportive of DNE (24) or LOF and GOF effects (25). This discrepancy is most likely due to the lack of intrinsic wild-type p53 expression in the cell lines used by Kotler et al. (25) compared to our study. Collectively, our findings demonstrate that the vast majority of *TP53* missense mutations occurring within its DNA-binding domain, including those recurrently found in myeloid malignancies, exert a strong DNE on wild-type p53's transcriptional activity, whereas missense mutations outside of the DNA-binding domain have either LOF or neutral effects.

Having studied the functional consequences of *TP53* missense mutations in isogenic AML cell line models *in vitro,* we sought to investigate the role of initiating *TP53* missense mutations on the response to DNA damage in hematopoietic stem and progenitor cells (HSPCs) *in vivo.* Pre-leukemic HSPCs carrying *TP53* mutations, including the missense mutations investigated in this study, undergo clonal selection after exposure to DNA-damaging chemotherapeutics (26) but the relative impact of specific *TP53* mutations is unknown. We generated mixed chimeric mice by transplanting HSPCs of various combinatorial genotypes derived from *Trp53* (gene nomenclature in mice is *Trp53* as opposed to *TP53* in humans) wild-type, *Trp53* knock-out and *Trp53* knock-in mice expressing the mouse homologs of R175H (R172H in mice) and R273H (R270H in mice) (10). We followed peripheral blood chimerism in sublethally irradiated and control mice over time to determine the *Trp53* genotype-specific relative competitive fitness upon DNA damage (Fig. 4A). As expected, $Trp53^{-/-}$ HSPCs had a strong competitive advantage over $Trp53^{+/+}$ or $Trp53^{+/-}$ HSPCs following sublethal irradiation, whereas $Trp53^{+/-}$ HSPCs expanded only modestly relative to $Trp53^{+/+}$ HSPCs (Fig. 4B). $Trp53^{+/+}$ HSPCs expressing congenic markers CD45.1 or CD45.2 had no competitive difference (Fig 4B, rightmost panel). The competitive advantage of $Trp53^{R172H/+}$ or $Trp53^{R270H/+}$ over $Trp53^{+/+}$ HSPCs was similar in magnitude to the competitive advantage of $Trp53^{-/-}$ over $Trp53^{+/+}$ HSPCs (Fig. 4B, C, D leftmost). Importantly, $Trp53^{R172H/+}$ or $Trp53^{R270H/+}$ outcompeted $Trp53^{+/-}$ HSPCs (Fig. 4C, D second from left). In contrast, $Trp53^{R172H/-}$ or $Trp53^{R270H/-}$ HSPCs displayed no competitive advantage over $Trp53^{-/-}$ HSPCs (Fig. 4C, D rightmost). These results demonstrate that these p53 missense variants exert a DNE on wild-type p53 upon DNA damage, leading to expansion of HSPCs *in vivo* in mice. We noted slight increases in chimerism even in non-irradiated control mice. However, these reached plateaus and were therefore interpreted as post-transplant fluctuations. Importantly, the results do not support a model in which the missense variants confer a GOF on p53 in mice. Interestingly, $Trp53^{R172H/+}$ or $Trp53^{R270H/+}$ HSPCs had a competitive disadvantage relative to $Trp53^{-/-}$ HSPCs (Fig. 4C, D second from right), which reveals that the DNE is incomplete *in vivo*, leading to residual wild-type p53 activity. This finding is consistent with the ongoing selective pressure to inactivate the remaining wild-type allele in patients with heterozygous missense mutations (6). Collectively, the various possible configurations of *Trp53* alleles in biallelic HSPCs result in a graded decrease in p53 activity that is paralleled by an increased resistance to genotoxic stress (Fig. 4E).

To examine whether our results are consistent with clinical observations, we investigated the association of *TP53* mutation type on clinical outcomes in AML patients. We analyzed a cohort of 164 patients with *TP53*-mutant AML from the German-Austrian AML Study Group (AMLSG) that had received intensive, anthracycline-/cytarabine-based chemotherapy. Consistent with the well-known *TP53* mutational spectrum, the vast majority of patients (n=137) had missense mutations, most of which (95.3%) were located within the DNA-binding domain (Fig. S12A). A small number of patients (n=27) had truncating mutations comprising frame-shift, nonsense, or splice mutations and these mutations were evenly distributed across the gene (Fig. S12A). An oncogenic p53 GOF in AML would be predicted to result in a more aggressive disease and worse survival outcomes in patients with missense mutations compared with patients who harbor truncating mutations. We found that AML

patients with missense mutations did not have a more aggressive disease than those with truncating mutations (Fig. S12B) and observed no significant difference in event-free (p=0.35) or overall (p=0.92) survival in patients bearing *TP53* missense or truncation mutations (Fig. 4F, G). In the subset of 101 patients (n=87 missense mutations, n=14 truncating mutations) for which co-mutation data were available (Fig. S13A), we did not observe statistically significant differences in the number of co-mutations per patient. Co-mutations were present in 7/14 (50%) and 42/87 (48.3%) of AML patients with *TP53* truncating or missense mutations, respectively (p=0.9999, Fisher's exact test). There was no evidence for a more aggressive co-mutational pattern in AML patients with *TP53* and the frequency of complex karyotype was not significantly different in patients with *TP53* missense mutations or truncating mutations. Overall, the outcomes of AML patients with *TP53* mutations in this dataset do not support the hypothesis that a putative mutant p53-mediated GOF causes a worse outcome in patients with *TP53* missense mutations.

In aggregate, phenotypic and functional analyses in isogenic human AML cell line models, *in vivo* functional studies in mice, and analysis of clinicogenomic data from AML patients consistently indicate that *TP53* missense mutations have dominant-negative activity without evidence of GOF capacity. We therefore propose a model in which missense variants exert a DNE that shapes the mutational spectrum early in the development of myeloid malignancies, often still at the pre-malignant stage (27-30), thereby providing a clonal reservoir of cells that are prone to expand and acquire secondary mutations resulting in development of myeloid malignancies. The concordance of the *TP53* mutational spectrum between pre-malignant clonal hematopoiesis of indeterminate potential (CHIP) and AML (Fig. S12A) suggests no major selective pressures for specific *TP53* mutations during disease progression into AML. Similar observations have been made in studies comparing pre-malignant lesions and overt cancer of the skin and esophagus (31, 32). Notably, the nearly identical *TP53* mutational spectrum in myeloid malignancies and solid tumors strongly suggest similar selection processes in many if not most cancers. Previous studies have demonstrated mutant p53 GOF mechanisms in epithelial cancers, implicating novel protein- protein interactions with other transcription factors including p63, NF-Y, NRF2 and ETS2 (11, 14, 15, 33). The discrepancy between our study and prior studies may be explained by distinct expression levels of these transcription factors in epithelial as compared to hematopoietic cells. For p63, a p53 family member, variable expression predominantly in epithelial tissues has indeed been reported (34), suggesting that GOF may be context-dependent (35).

In summary, our studies demonstrate that in myeloid malignancies *TP53* missense mutations do not lead to novel GOF activities but instead drive clonal selection through dominant-negative effects. Future studies aimed at elucidating the molecular mechanisms of the DNE may lead to therapeutic strategies that prevent outgrowth of *TP53*-mutant clones and progression into AML and MDS.

Supplementary Material

Refer to Web version on PubMed Central for supplementary material.

ACKNOWLEDGMENTS

We thank A. S. Sperling, R. S. Sellar, and M. Slabicki for critical review of the manuscript.

Funding: B.L.E. and S.A.A. received funding from the NIH (P01CA066996, P50CA206963, and R01HL082945). B.L.E was funded from the Howard Hughes Medical Institute, the Edward P. Evans Foundation, the Leukemia and Lymphoma Society, the Adelson Medical Research Foundation, and the Henry and Marilyn Taub Foundation. S.B. was supported by fellowships from the Swiss Cancer League (KLS-3625-02 2015) and Swiss National Science Foundation (P300PB_161026/1 and P400PM_183862). K.J.K was supported by Jane and Aatos Erkko Foundation, Orion Research Foundation, and Instrumentarium Science Foundation. This work was supported in part by U01 CA176058 (W.C.H.) and U01 CA199253 (W.C.H., T.J.).

REFERENCES AND NOTES

1. Levine AJ, Oren M, The first 30 years of p53: growing ever more complex. Nat. Rev. Cancer 9, 749–758 (2009). [PubMed: 19776744]
2. Bejar R et al., Clinical effect of point mutations in myelodysplastic syndromes. N. Engl. J. Med 364, 2496–2506 (2011). [PubMed: 21714648]
3. Rücker FG et al., TP53 alterations in acute myeloid leukemia with complex karyotype correlate with specific copy number alterations, monosomal karyotype, and dismal outcome. Blood. 119, 2114–2121 (2012). [PubMed: 22186996]
4. Lindsley RC et al., Prognostic Mutations in Myelodysplastic Syndrome after Stem-Cell Transplantation. N. Engl. J. Med 376, 536–547 (2017). [PubMed: 28177873]
5. Kastenhuber ER, Lowe SW, Putting p53 in Context. Cell. 170, 1062–1078 (2017). [PubMed: 28886379]
6. Liu Y et al., Deletions linked to TP53 loss drive cancer through p53-independent mechanisms. Nature. 531, 471–475 (2016). [PubMed: 26982726]
7. Brosh R, Rotter V, When mutants gain new powers: news from the mutant p53 field. Nat. Rev. Cancer 9, 701–713 (2009). [PubMed: 19693097]
8. Baugh EH, Ke H, Levine AJ, Bonneau RA, Chan CS, Why are there hotspot mutations in the TP53 gene in human cancers? Cell Death Differ. 25, 154–160 (2018). [PubMed: 29099487]
9. Dittmer D et al., Gain of function mutations in p53. Nat. Genet 4, 42–46 (1993). [PubMed: 8099841]
10. Olive KP et al., Mutant p53 Gain of Function in Two Mouse Models of Li-Fraumeni Syndrome. Cell. 119, 847–860 (2004). [PubMed: 15607980]
11. Di Agostino S et al., Gain of function of mutant p53: The mutant p53/NF-Y protein complex reveals an aberrant transcriptional mechanism of cell cycle regulation. Cancer Cell. 10, 191–202 (2006). [PubMed: 16959611]
12. Do PM et al., Mutant p53 cooperates with ETS2 to promote etoposide resistance. Genes Dev. 26, 830–845 (2012). [PubMed: 22508727]
13. Xu J et al., Gain of function of mutant p53 by coaggregation with multiple tumor suppressors. Nat. Chem. Biol 7, 285–295 (2011). [PubMed: 21445056]
14. Zhu J et al., Gain-of-function p53 mutants co-opt chromatin pathways to drive cancer growth. Nature. 525, 206–211 (2015). [PubMed: 26331536]
15. Walerych D et al., Proteasome machinery is instrumental in a common gain-of-function program of the p53 missense mutants in cancer. Nat. Cell Biol 18, 897–909 (2016). [PubMed: 27347849]
16. Srivastava S, Wang S, Tong YA, Hao ZM, Chang EH, Dominant negative effect of a germ-line mutant p53: a step fostering tumorigenesis. Cancer Res. 53, 4452–4455 (1993). [PubMed: 8402611]
17. Hegi ME et al., p53 transdominance but no gain of function in mouse brain tumor model. Cancer Res. 60, 3019–3024 (2000). [PubMed: 10850451]
18. de Vries A et al., Targeted point mutations of p53 lead to dominant-negative inhibition of wild-type p53 function. Proc. Natl. Acad. Sci. USA 99, 2948–2953 (2002). [PubMed: 11867759]
19. Lee MKet al., Cell-type, dose, and mutation-type specificity dictate mutant p53 functions in vivo. Cancer Cell. 22, 751–764 (2012). [PubMed: 23238012]

20. McGahon AJ et al., Downregulation of Bcr-Abl in K562 cells restores susceptibility to apoptosis: characterization of the apoptotic death. Cell Death Differ. 4, 95–104 (1997). [PubMed: 16465215]
21. Chylicki K et al., p53-mediated differentiation of the erythroleukemia cell line K562. Cell Growth Differ. 11, 315–324 (2000). [PubMed: 10910098]
22. Di Bacco AMA, Cotter TG, p53 expression in K562 cells is associated with caspase- mediated cleavage of c-ABL and BCR-ABL protein kinases. Br. J. Haematol 117, 588–597 (2002). [PubMed: 12028026]
23. Baker SJ, Markowitz S, Fearon ER, Willson JK, Vogelstein B, Suppression of human colorectal carcinoma cell growth by wild-type p53. Science. 249, 912–915 (1990). [PubMed: 2144057]
24. Giacomelli AO et al., Mutational processes shape the landscape of TP53 mutations in human cancer. Nat. Genet 50, 1–12 (2018). [PubMed: 29273803]
25. Kotler E et al., A Systematic p53 Mutation Library Links Differential Functional Impact to Cancer Mutation Pattern and Evolutionary Conservation. Mol. Cell 71, 178–190.e8 (2018). [PubMed: 29979965]
26. Wong TN et al., Role of TP53 mutations in the origin and evolution of therapy-related acute myeloid leukaemia. Nature. 518, 552–555 (2015). [PubMed: 25487151]
27. Jaiswal S et al., Age-Related Clonal Hematopoiesis Associated with Adverse Outcomes. N. Engl. J. Med 26, 2488–2498 (2014).
28. Genovese G et al., Clonal Hematopoiesis and Blood-Cancer Risk Inferred from Blood DNA Sequence. N. Engl. J. Med 26, 2477–2487 (2014).
29. Abelson S et al., Prediction of acute myeloid leukaemia risk in healthy individuals. Nature. 559, 1–23 (2018).
30. Desai P et al., Somatic mutations precede acute myeloid leukemia years before diagnosis. Nat. Med 24, 1–12 (2018). [PubMed: 29315299]
31. Martincorena I et al., High burden and pervasive positive selection of somatic mutations in normal human skin. Science. 348, 880–886 (2015). [PubMed: 25999502]
32. Martincorena I et al., Somatic mutant clones colonize the human esophagus with age. Science. 362, 911–917 (2018). [PubMed: 30337457]
33. Adorno M et al., A Mutant-p53/Smad complex opposes p63 to empower TGFbeta-induced metastasis. Cell. 137, 87–98 (2009). [PubMed: 19345189]
34. Di Como CJ et al., p63 expression profiles in human normal and tumor tissues. Clinical Cancer Res. 8, 494–501 (2002). [PubMed: 11839669]
35. Kim MP, Lozano G, Mutant p53 partners in crime. Cell Death Differ. 25, 161–168 (2018). [PubMed: 29099488]

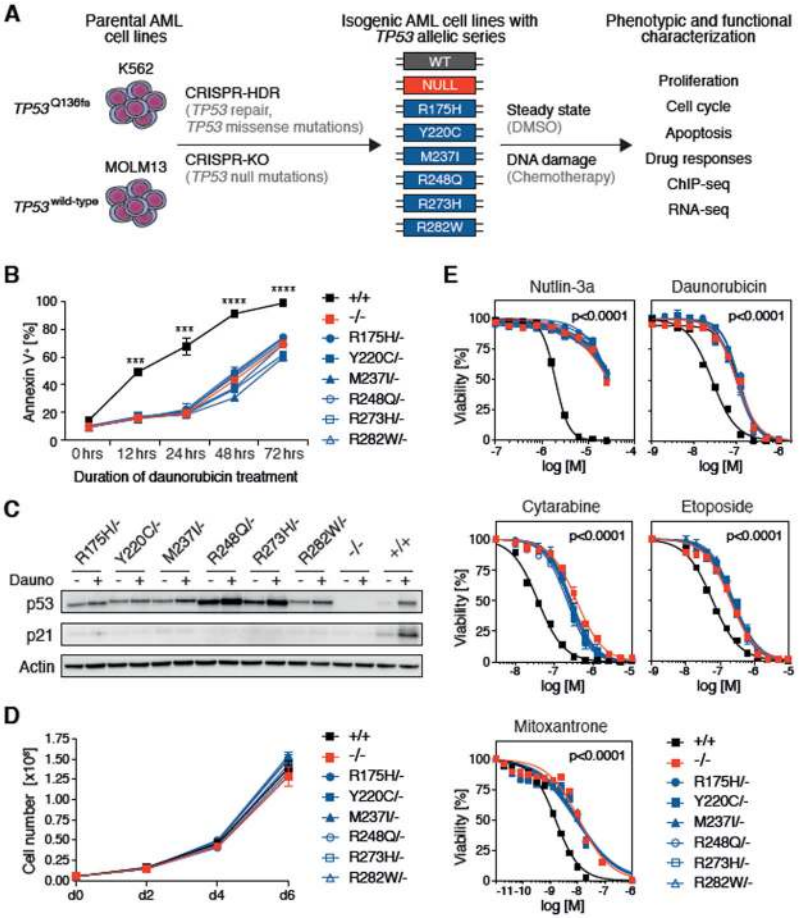

Fig. 1. TP53 hotspot missense and null mutations in isogenic AML cell lines show similar oncogenic phenotypes.

(**A**) Schematic of the experimental workflow for generating K562-*TP53* and MOLM13-*TP53* isogenic AML cell lines. CRISPR-HDR, CRISPR-Cas9-mediated homology-directed repair; CRISPR-KO, CRISPR-Cas9-mediated gene knock-out (**B**) MOLM13-*TP53* isogenic AML cell lines were treated with 100nM daunorubicin for up to 72 hours. At the indicated time points, cells were stained with Annexin V and analyzed by flow cytometry to assess total apoptotic cells (replicates n=3, symbols represent averages of experimental replicates, error bars indicate s.e.m., *** $p<0.001$, **** $p<0.0001$, two-tailed Student's *t*-test). (**C**) MOLM13-*TP53* isogenic AML cell lines were treated with DMSO (−) or 100nM daunorubicin (+) for 6 hours, after which whole cell protein lysates were collected, run on a polyacrylamide gel, and immunoblotted for p53, p21 and actin (replicates n=3, representative images are shown). (**D**) Growth kinetics of MOLM13-*TP53* isogenic AML cell lines (replicates n=3, symbols represent averages of experimental replicates, error bars indicate s.e.m.). (**E**) MOLM13-*TP53* isogenic AML cell lines were treated with DMSO or indicated drugs at increasing concentrations for 72 hours, after which cell viability was assessed using CellTiter-Glo® luminescent assay, (replicates n=3, symbols represent averages of experimental replicates, error bars indicate s.e.m.).

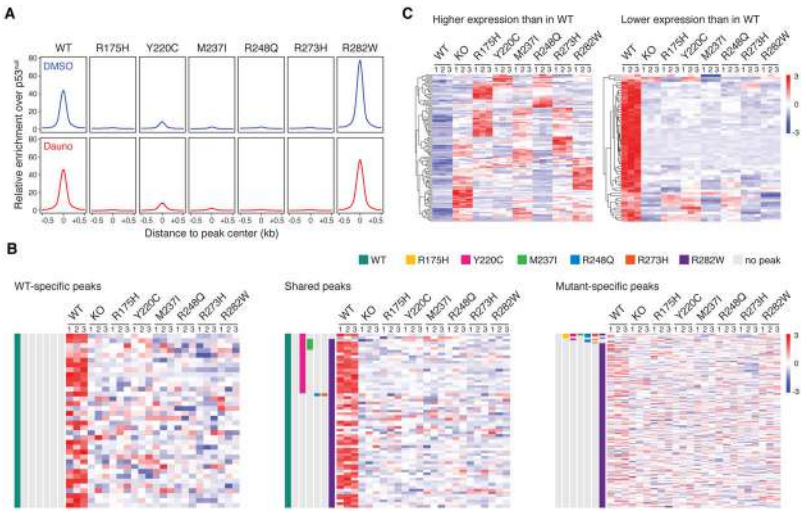

Fig. 2. Transcriptional consequences of *TP53* hotspot missense mutations in isogenic AML cell lines.

(**A**) Genome-wide relative enrichment of wildtype and missense mutant p53 variants (ChIP for wild-type or missense mutant p53 over ChIP in $p53^{-/-}$ cells) over transcriptional start site (TSS)-proximal regions (−10kb – first intron) in K562-*TP53* isogenic cell lines upon treatment with DMSO or 100nM daunorubicin for 24 or 6 hours, respectively. (**B**) Heatmap depicting normalized expression of genes associated with WT-specific (left), shared (middle), and p53 mutant-specific (right) ChIP-seq peaks in K562-*TP53* isogenic cell lines treated with 100nM daunorubicin for 24 hours (experimental replicates n=3). (**C**) Heatmap of the pooled top 30 (left) and pooled bottom 30 (right) genes relative to wild-type p53 in K562-*TP53* isogenic cell lines treated with 100nM daunorubicin for 24 hours (RNA-seq experimental replicates n=3).

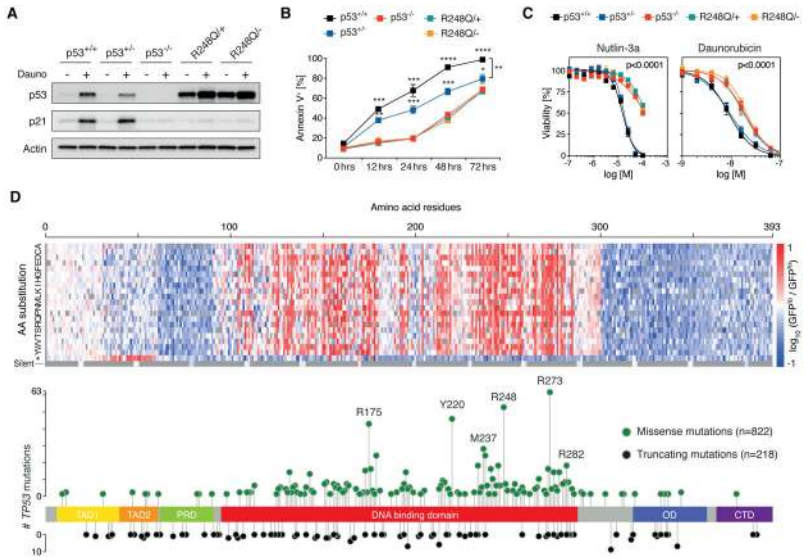

Fig. 3. *TP53* missense mutations within the DNA-binding domain confer dominant-negative effects.

(**A**) MOLM13-*TP53* isogenic AML cell lines with $p53^{+/+}$, $p53^{+/-}$, $p53^{-/-}$ as well as $p53^{R248Q/+}$ and $p53^{R248Q/-}$ were treated with DMSO (–) or 100nM daunorubicin (+) for 6 hours, after which whole cell protein lysates were collected, run on a polyacrylamide gel, and immunoblotted for p53, p21 and actin (replicates n=3, representative images are shown). (**B**) MOLM13-*TP53* isogenic AML cell lines were treated 100nM daunorubicin for up to 72 hours. At the indicated time points, cells were stained with Annexin V and analyzed by flow cytometry to assess total apoptotic cells (replicates n=3, symbols represent averages of experimental replicates, error bars indicate s.e.m., * p,0.05, **p,0.01, ***p<0.001, **** p<0.0001, two-tailed Student's *t*-test). (**C**) MOLM13-*TP53* isogenic AML cell lines were treated with DMSO, nutlin-3a or daunorubicin at increasing concentrations for 72 hours, after which cell viability was assessed using CellTiter-Glo® luminescent assay. (replicates n=3, symbols represent averages of experimental replicates, error bars indicate s.e.m.). (**D**) Heatmap depicting the *TP53* saturation mutagenesis screen results after nutlin-3a treatment shown as log10 of the ratio of normalized read counts in GFP^{lo} over GFP^{hi} cells per *TP53* variant (top panel) overlaid on a lollipop plot demonstrating *TP53* mutational data from 1,040 patients with myelodysplastic syndromes (MDS), myeloproliferative neoplasms (MPN), and AML (bottom panel). Missense mutations (green circles) and truncating mutations (black circles) comprising frame-shift, nonsense, and splice mutations are shown. TAD, transactivation domain; PRD, proline-rich domain; OD, oligomerization domain; CTD, C-terminal domain.

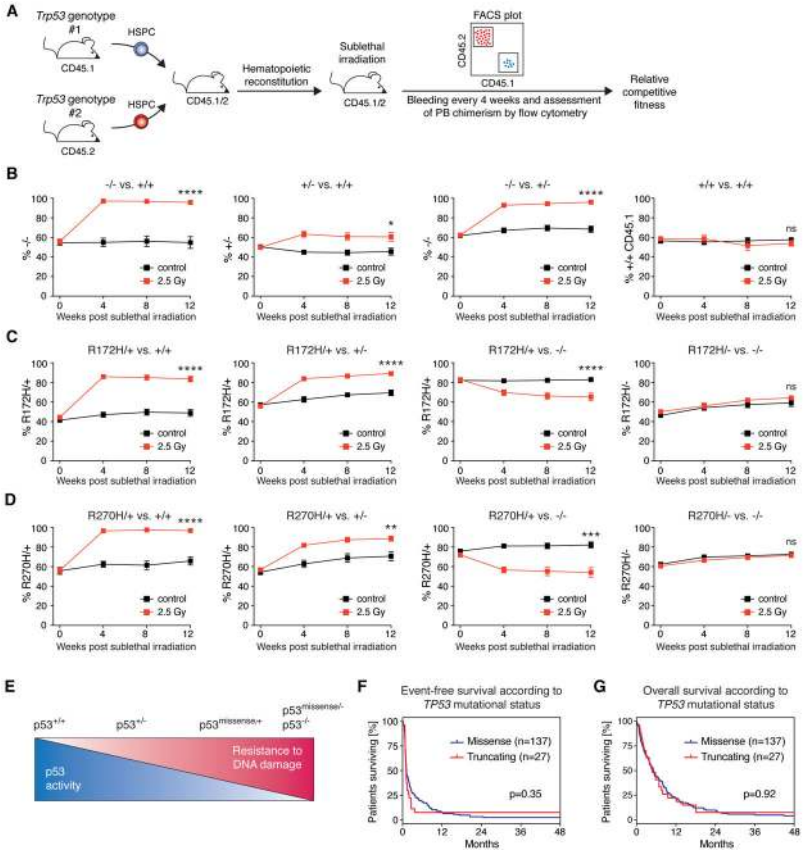

Fig. 4. Heterozygous *Trp53* missense mutations confer a competitive advantage over *Trp53*$^{+/-}$ HSPCs upon sublethal gamma-irradiation.

(**A**) Schematic of the experimental workflow for hematopoietic competition assays in mixed chimeric mice to assess the relative competitive fitness of *Trp53* genotypes upon sublethal gamma-irradiation. *Trp53*$^{+/+}$-CD45.1/2 recipient mice were engrafted with a 1:1 mixture of *Trp53* genotypes from either CD45.1 or CD45.2 mice. Following hematopoietic reconstitution, mixed chimeric mice were sublethally gamma-irradiated (single dose of 2.5 Gy), and thereafter, peripheral blood (PB) chimerism was assessed by flow-cytometry every 4 weeks. (**B-D**) PB chimerism in mixed chimeric mice of the indicated genotypes in non-irradiated control mice (black squares) and mice treated with a single dose of 2.5 Gy gamma-irradiation (red squares). (experimental replicates n=2-3 per group, n=14-20 mice per group, symbols represent averages of individual mice across experimental replicates, error bars indicate s.e.m., * p<0.05, ** p<0.01, *** p<0.001, **** p<0.0001, Mann-Whitney test) (**E**) Schematic summary of the results obtained from hematopoietic competition assays depicting the relative competitive fitness of the indicated *Trp53* genotypes towards sublethal DNA damage. (**F**) Kaplan-Meier analysis for event-free and (**G**) overall survival in AML patients according to *TP53* mutational status (missense mutations, blue line or truncating mutations comprising frame-shift, nonsense, and splice mutation, red line, log-rank (Mantel-Cox) test).